Neutralizing Effect of Synthetic Peptides toward SARS-CoV-2

Pedro F.N. Souza,* Maurício F. vanTilburg, Felipe P. Mesquita, Jackson L. Amaral, Luina B. Lima, Raquel C. Montenegro, Francisco E.S. Lopes, Rafael X. Martins, Leonardo Vieira, Davi F. Farias, Ana C. O. Monteiro-Moreira, Cleverson D.T. Freitas, Arnaldo S. Bezerra, Maria I. F. Guedes, Débora S.C.M. Castelo-Branco, and Jose T.A. Oliveira

Cite This: *ACS Omega* 2022, 7, 16222−16234

Read Online

ACCESS | Metrics & More | Article Recommendations | Supporting Information

ABSTRACT: The outbreak caused by SARS-CoV-2 has taken many lives worldwide. Although vaccination has started, the development of drugs to either alleviate or abolish symptoms of COVID-19 is still necessary. Here, four synthetic peptides were assayed regarding their ability to protect Vero E6 cells from SARS-CoV-2 infection and their toxicity to human cells and zebrafish embryos. All peptides had some ability to protect cells from infection by SARS-CoV-2 with the D614G mutation. Molecular docking predicted the ability of all peptides to interact with and induce conformational alterations in the spike protein containing the D614G mutation. PepKAA was the most effective peptide, by having the highest docking score regarding the spike protein and reducing the SARS-CoV-2 plaque number by 50% (EC_{50}) at a concentration of 0.15 mg mL^{-1}. Additionally, all peptides had no toxicity to three lines of human cells as well as to zebrafish larvae and embryos. Thus, these peptides have potential activity against SARS-CoV-2, making them promising to develop new drugs to inhibit cell infection by SARS-CoV-2.
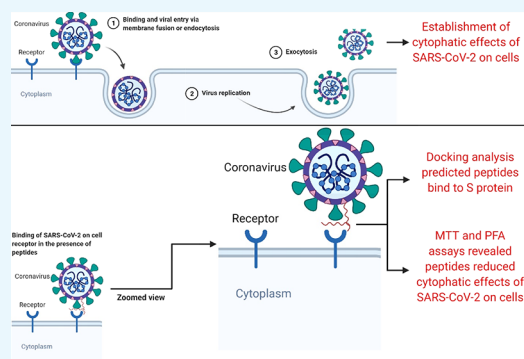
INTRODUCTION

The outbreak of the coronavirus disease in late 2019 (COVID-19) is still ongoing and has already claimed more than 4 million lives worldwide.[1,2] The causative agent of COVID-19 was later identified as SARS-CoV-2 (Severe Acute Respiratory Syndrome Coronavirus 2), which is 96 and 79% similar, respectively, to BatCoV RatG13 (a coronavirus from bats) and another pandemic coronavirus, SARS-CoV.[3] Coronaviruses are a group of viruses belonging to the family *Coronaviridae*, a group of enveloped positive-stranded RNA viruses with both medical and veterinary importance. The RNA genome produces a larger polyprotein composed of non-structural (NSPs) and structural proteins (SPs). The NSPs are classified from 1 to 16 and the SPs are identified as spike (S), envelope (E), membrane (M), and nucleocapsid (N) proteins.[4]

Due to the huge effort of scientists worldwide, an unprecedented breakthrough was achieved. In less than a year, vaccination campaigns began in virtually all countries.[5] However, two problems have arisen: (1) the rate of vaccination is not fast enough to reach herd immunity worldwide, and (2) countries with low vaccination rates are a repository of SARS-CoV-2 mutants that threaten the efficacy of the vaccines, causing vaccinated people to be jeopardized by COVID-19.[4,6] Most of the mutations in the SARS-CoV-2 genome are concentrated in the RBD domain of S protein. S protein is the main focus of most vaccines developed, so mutations on it could reduce their

efficacy.[6] Other points are that poor countries that cannot afford to buy vaccines are still struggling with COVID-19, and the development of specific drugs for clinical treatment of the symptoms is still necessary. Therefore, the development of drugs for COVID-19, despite the availability of vaccines, is still urgent.[7] Drug repositioning has been employed to accelerate the process of drug development. This entails testing drugs already approved for the treatment of other diseases against SARS-CoV-2. Despite reaching good results in computational simulations, in vitro tests have so far revealed the inefficiency of the targeted drugs.[7]

In this context, in two previous studies, our research group employed computational simulations to drive antimicrobial peptides toward the S protein[8] and Mpro[9] of SARS-CoV-2. In the first study, Souza et al.[8] reported that out of 8 peptides, two peptides, *Mo*-CBP$_3$-PepII and PepKAA, strongly bonded to the S protein, leading to changes in structural conformation and interaction with the ACE2 receptor. In the second study, Amaral et al.[9] employed the same peptides against Mpro. Of these, three
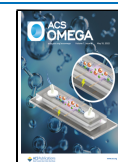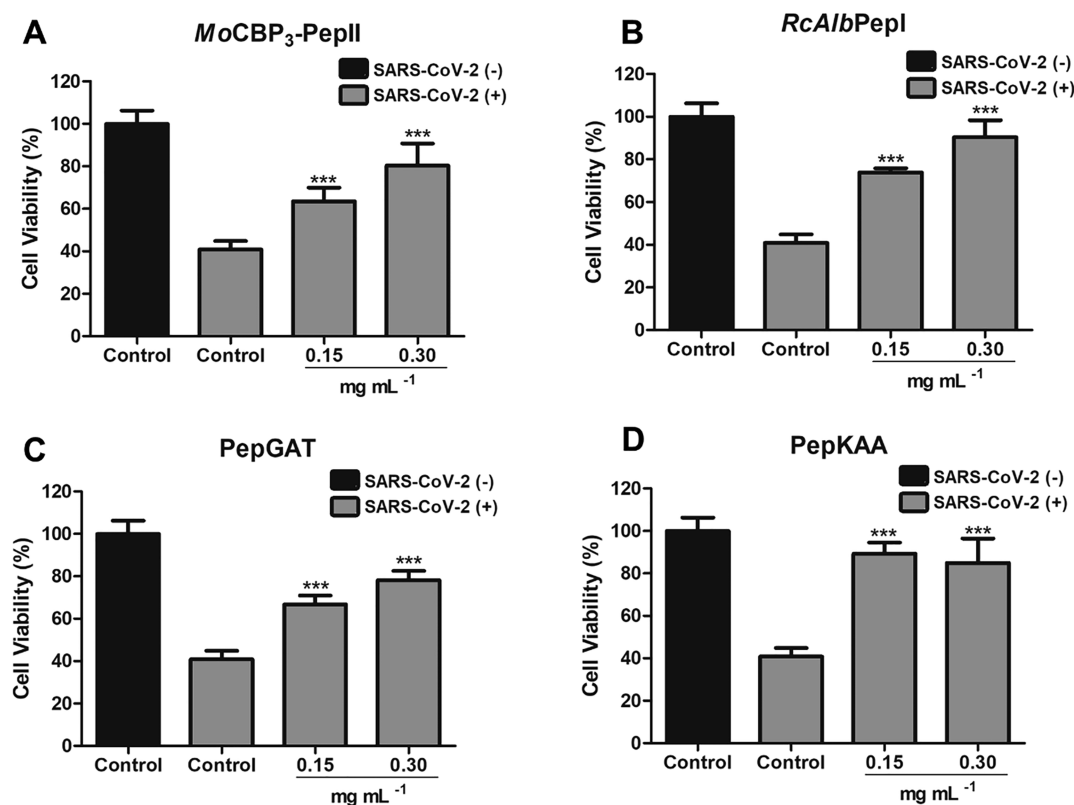
Figure 1. Inhibitory activity of synthetic peptides against SARS-CoV-2 infection. (A) Mo-CBP3-PepII, (B) RcAlb-PepI, (C) PepGAT, and (D) PepKAA inhibiting Vero E6 cell infection by SARS-CoV-2 as revealed by MTT assay for cell viability. Peptides at different concentrations were incubated with SARS-CoV-2 for 30 min; then, SARS-CoV-2 was mixed with Vero E6 cells for 4 h. After that, cells were incubated for 96 h, and cell viability was evaluated by MTT assay. Vero E6 cells with and without SARS-CoV-2 infection were used as controls for cell viability. Data are shown as mean ± standard deviation of three independent experiments. ***$P < 0.001$. The neutralizing effect of peptides against SARS-CoV-2.

peptides, RcAlb-PepI, PepGAT, and PepKAA, interacted the best with Mpro, leading to conformational changes and reduction in the catalytic site. The results of both studies suggested that those peptides could have anti-SARS-CoV-2 action in vitro, making them potential candidates for the development of a specific drug to treat COVID-19 symptoms.

The four peptides tested here were designed from plant proteins.[10−12] Mo-CBP3-PepII and RcAlb-PepI were designed, respectively, from a chitin-binding protein of *Moringa oleifera* and a 2S albumin of *Ricinus communis*.[10,11] PepGAT and PepKAA were designed from a chitinase from *Arabidopsis thaliana*.[12] All peptides are positively charged, have hydrophobic ratio from 40 to 65%, were predicted to have antiviral action, and are resistant to intestinal enzymes, indicating the potential for oral administration.[10−12] Here, we report the in vitro activity of those peptides against SARS-CoV-2 in addition to their level of toxicity.

■ RESULTS

Anti-SARS-CoV-2 Potential of Synthetic Peptides. To test whether the peptides can suppress virus-induced cytopathic effects, a simple and fast MTT [3-(4,5-dimethylthiazol-2-yl)-2,5-diphenyltetrazolium] bioassay for screening drugs against SARS-CoV-2 was used. The MTT assay is a simple colorimetric test to assess cell metabolic activity in a microplate reader. It is based on the activity of the NAD(P)H-dependent cellular oxidoreductase, which transforms the tetrazolium bromide from MTT into formazan, which has a purple color, allowing the determination of presence of the number of viable cells.[13] Based

on that, we expected that the cells infected by SARS-CoV-2 would not convert the MTT into formazan because they had been killed by SARS-CoV-2, and the control cells (without SARS-CoV-2 exposure) would convert all MTT into formazan because they would be metabolically active (Figure 1).

All peptides were able to inhibit virus-induced cytopathic effects, with EC_{50} values in the microgram/milliliter range (Table 1). Thus, we performed a test with a fixed concentration

Table 1. EC50 Values for Peptides Treatment in Vero E6 Cell Culture Infected with SARS-CoV-2[a]

peptides	EC50 (mg mL^{-1})	CI95%
MoCBP3-PepII	0.09	0.04−0.19
RcAlbPepI	0.05	0.03−0.07
PepGAT	0.08	0.07−0.09
PepKAA	0.04	0.02−0.07

[a]EC50: concentration of a drug that gives a half-maximal response. CI95%: 95% confidence interval.

to investigate the inhibition of virus-induced cytopathic effects at 0.15 and 0.30 mg mL^{-1}. The positive control cells [exposed to dimethyl sulfoxide (DMSO)] presented 100% viability, while the cells infected with SARS-CoV-2 presented about 40% viability (Figure 1). At 0.15 mg mL^{-1}, the peptides Mo-CBP3-PepII, RcAlb-PepI, PepGAT, and PepKAA reduced the SARS-CoV-2 cytopathic effects by 60, 75, 65, and 90%, respectively (Figure 1). At 0.30 mg mL^{-1}, the reductions of SARS-CoV-2 cytopathic effects were 75, 90, 85, and 80%, respectively, for Mo-
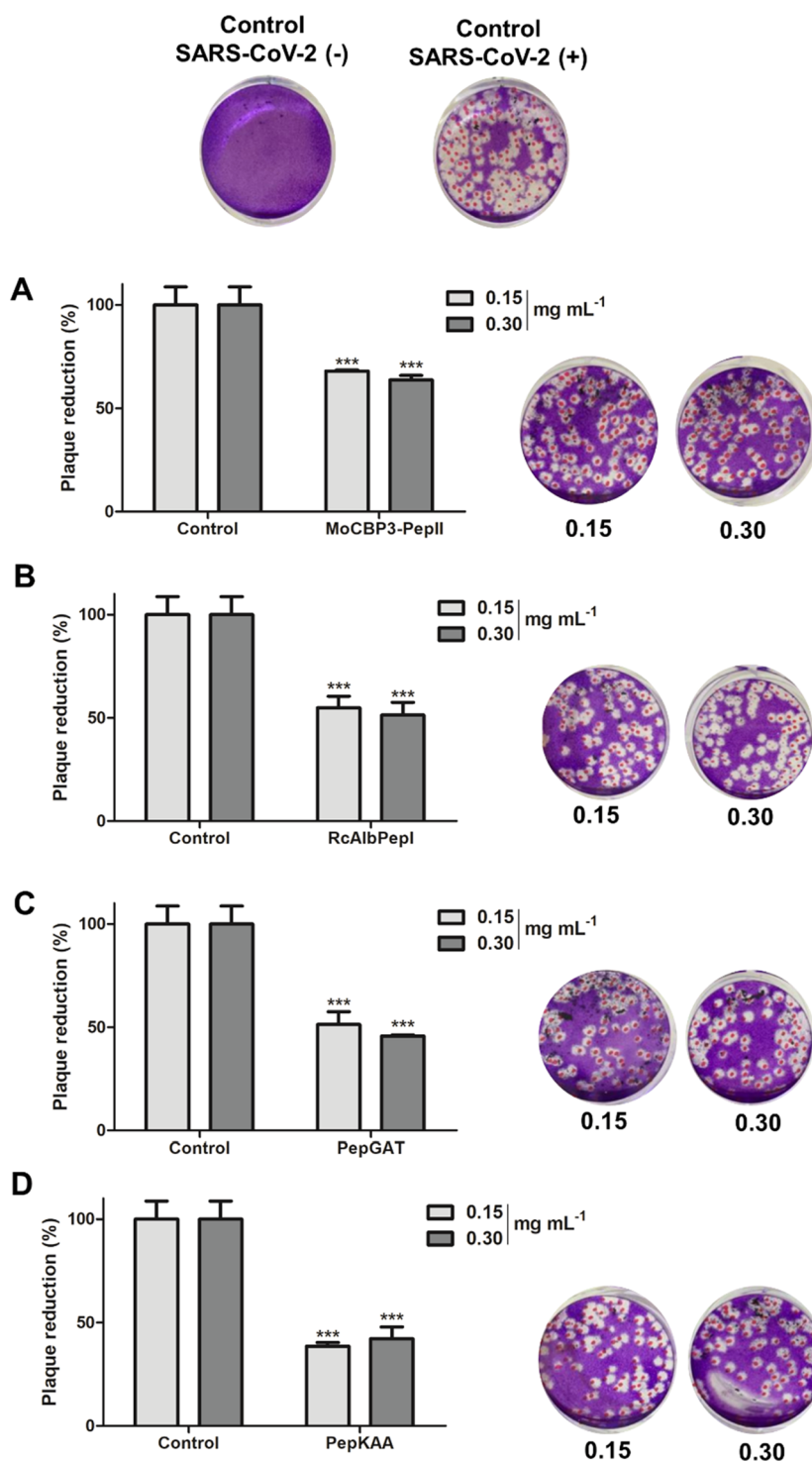
Figure 2. Plaque reduction neutralization effect of synthetic peptides against SARS-CoV-2. (A) *Mo*-CBP3-PepII, (B) *Rc*Alb-PepI, (C) PepGAT, and (D) PepKAA inhibiting SARS-CoV-2 plaque formation on Vero E6 cells. One hundred PFU of SARS-CoV-2 were incubated with the peptides at different at 37 °C for 1 h. Then, they were added to pre-seeded Vero E6 cells at 90−100% confluence. After fixation for 1 h, the overlay was removed, and cells were stained with 0.5% crystal violet. Vero E6 cells with and without SARS-CoV-2 were used as negative controls for SARS-CoV-2 neutralization. Data are shown as mean $\pm$ standard deviation of three independent experiments. ***$P < 0.001$.

CBP3-PepII, *RcAlb*-PepI, PepGAT, and PepKAA (Figure 1). The best peptides and concentrations were PepKAA at 0.15 mg mL^{-1} and *RcAlb*-PepI at 0.30 mg mL^{-1}, in both cases reaching 90% cell viability.

To confirm the neutralizing effect of peptides against SARS-CoV-2, the peptides were first incubated with SARS-CoV-2 and then added to a Vero E6 cell monolayer. All tested peptides (0.15 and 0.30 mg mL^{-1}) significantly reduced the plaque formation in Vero E6 cell co-cultures with SARS-CoV-2 (Figure 2). The least effective peptide was *Mo*-CBP3-PepII, which inhibited plaque formation only by about 35 at both concentrations (Figure 2A). In turn, the most effective peptide was PepKAA, which achieved inhibition of around 60% at both concentrations (Figure 2D).
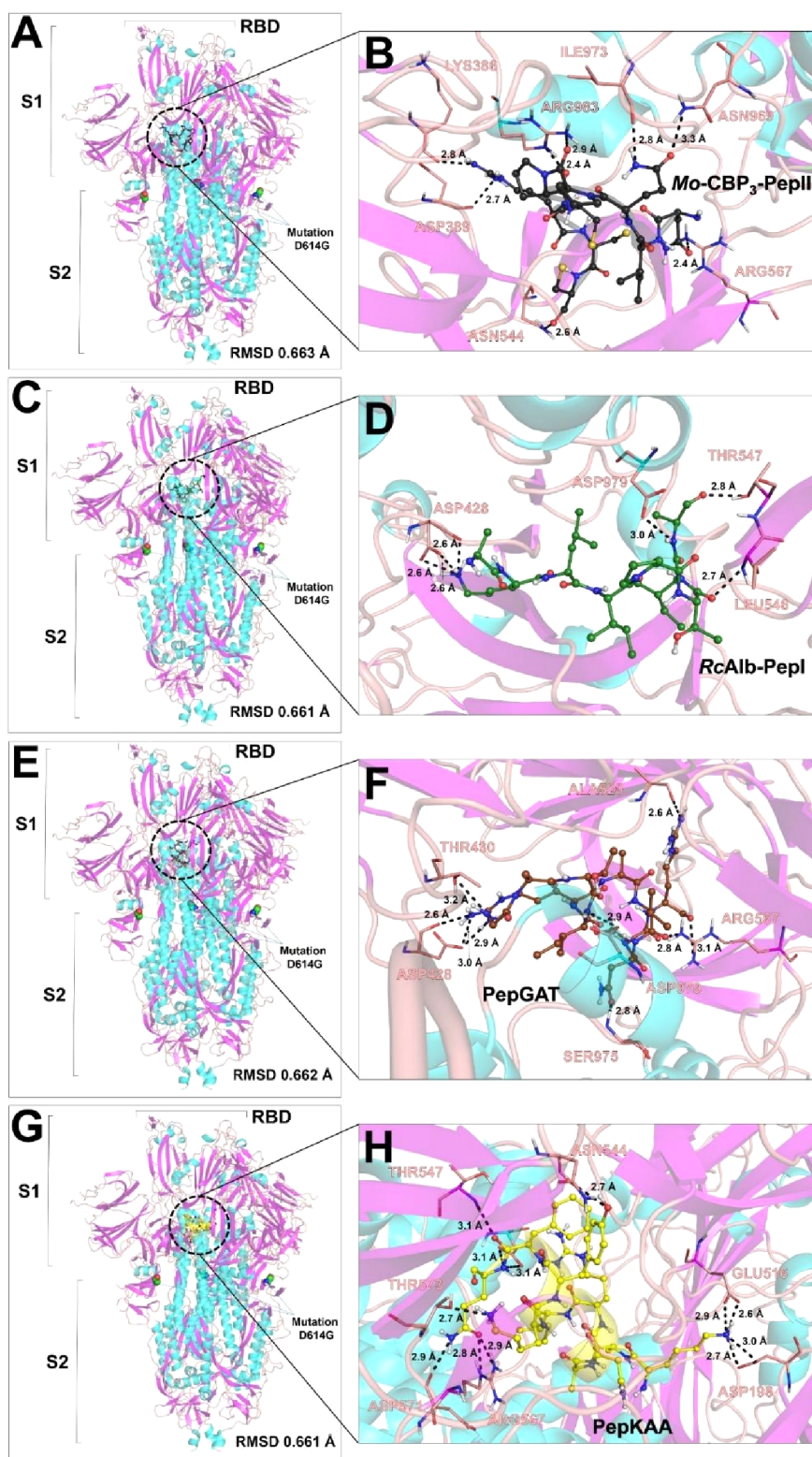
Figure 3. Peptides Mo-CBP$_3$-PepII, RcAlb-PepI, PepGAT, and PepKAA interacting with the mutated S protein (S^{D614G}) of SARS-CoV-2. (A,C,E,G) General view of the interaction between S^{D614G} with Mo-CBP$_3$-PepII, RcAlb-PepI, PepGAT, and PepKAA, respectively. (B,D,F,H) Zoomed overview of the interaction and the hydrogen bonds between S^{D614G} and peptides Mo-CBP$_3$-PepII, RcAlb-PepI, PepGAT, and PepKAA, respectively. Toxicity of peptides to human cells.

Molecular Docking of Peptides toward the D614G Mutant of S Protein. The results of a recent study[8] revealed that all peptides tested interacted with the S protein from the Wuhan isolate of SARS-CoV-2. Of these, Mo-CBP$_3$-PepII and

PepKAA presented the strongest interaction energies.[8] In our study, sequencing revealed that the SARS-CoV-2 isolate contained D614G on the S protein (Figure S1). Thus, we
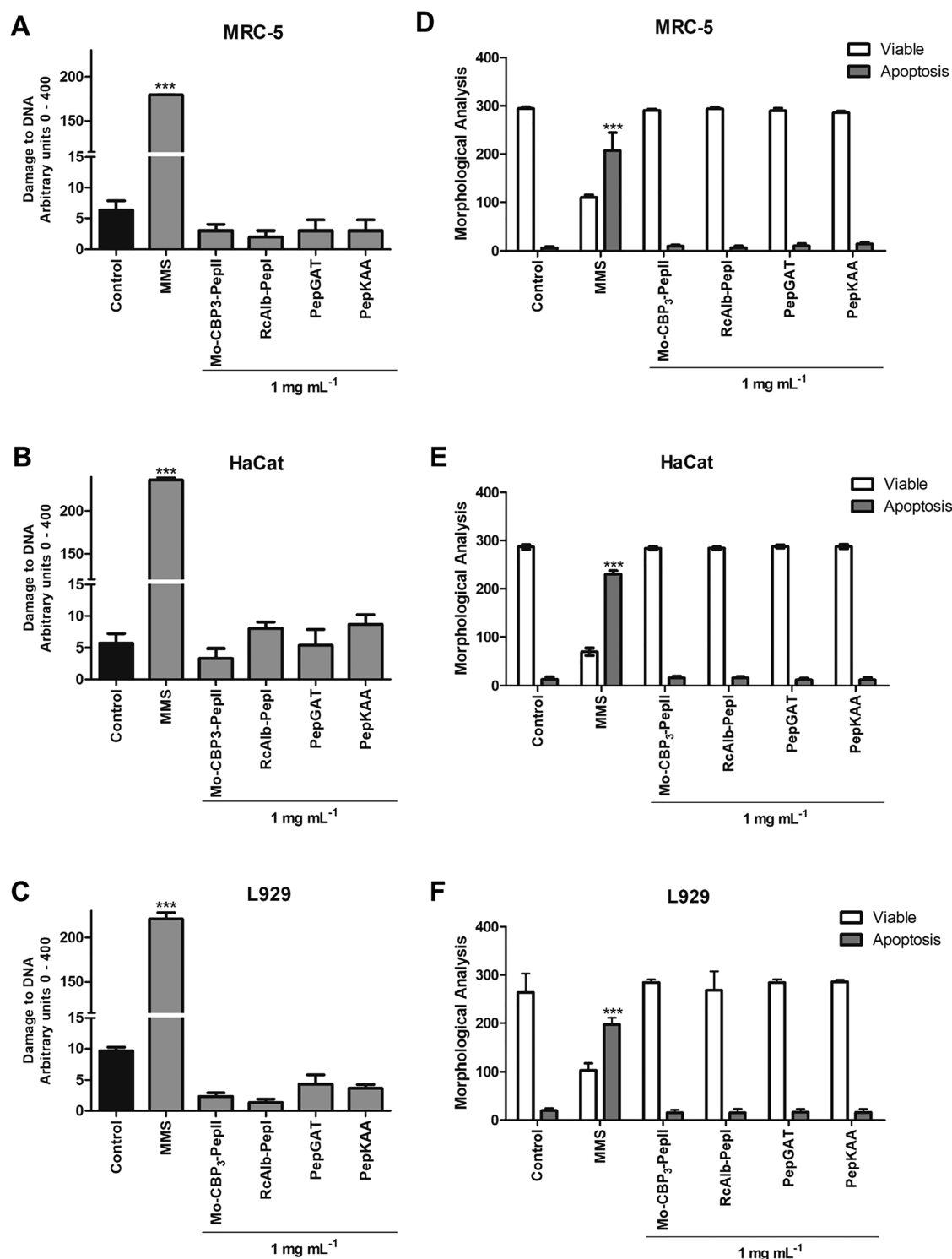
Figure 4. Assessment of toxicity of *Mo*-CBP$_3$-PepII, *Rc*Alb-PepI, PepGAT, and PepKAA to human cell lines. (A) L929, (B) HaCat, and (C) MRC-5 lines were incubated with synthetic peptides at a concentration of 1 mg mL to evaluate the damage to DNA by comet assay. (D−F) Cell lines were incubated with peptides as described and evaluated for viable cells and cells in apoptosis. MMS (4×10^{-5} M) was employed as a positive control for cell toxicity and healthy cells as a negative control for toxicity. Data are shown as mean ± standard deviation of three independent experiments. ***P < 0.001.

performed a new docking analysis to see if the peptides would still interact with this mutant protein.

The molecular docking analysis predicted that *Mo*-CBP$_3$-PepII, *Rc*Alb-PepI, PepGAT, and PepKAA would interact in the S1 region of the mutant protein S (D614G) of SARS-CoV-2 (Figure 3A,C,E,G). We observed alterations in the atomic

positions of the S protein after interaction with peptides, revealed by variations in RMSD values of 0.663, 0.661, 0.662, and 0.661 Å, respectively, to *Mo*-CBP$_3$-PepII, *Rc*Alb-PepI, PepGAT, and PepKAA.

Mo-CBP$_3$-PepII presented the lowest binding energy of interaction (LBEI), −676.1 kJ·mol^{-1} with S^{D614G}. The
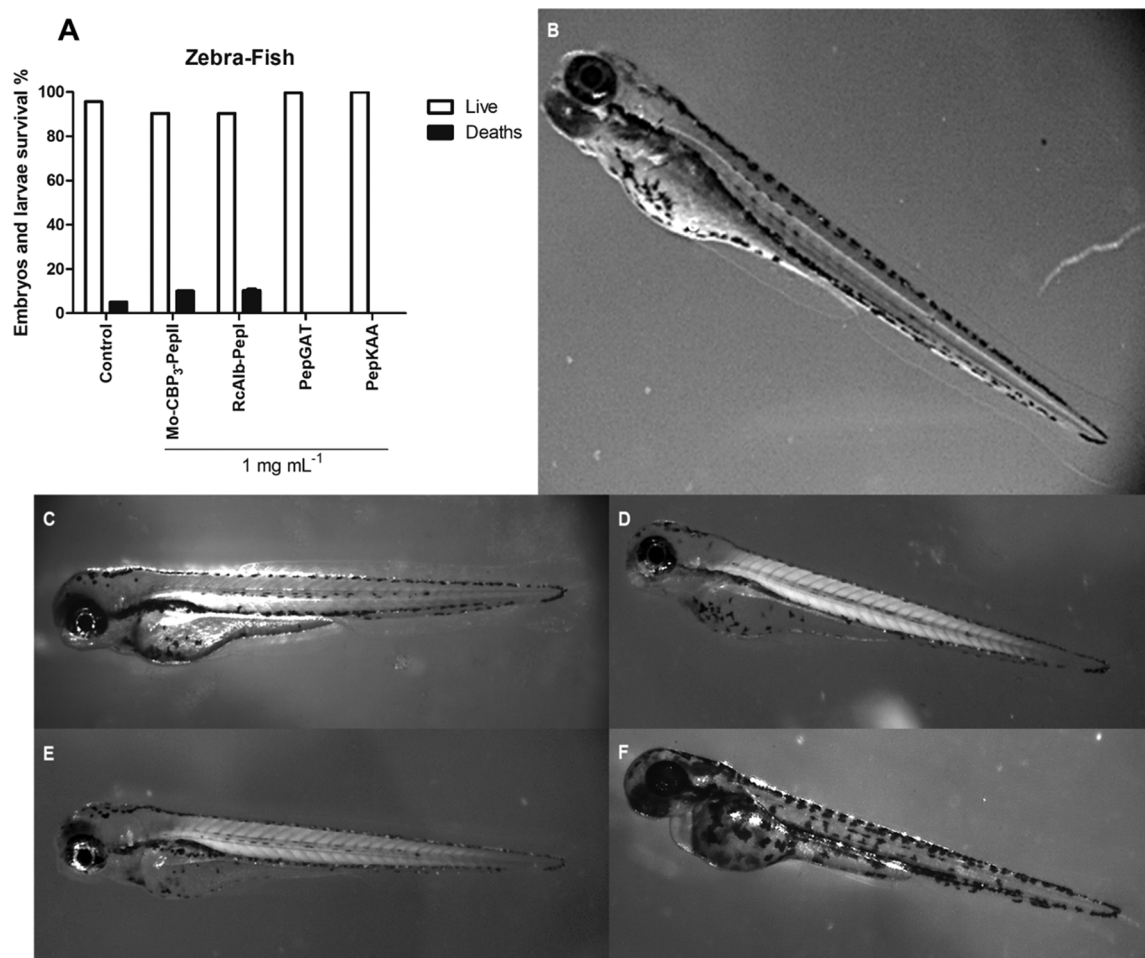
Figure 5. Assessment of toxicity of *Mo*-CBP$_3$-PepII, *Rc*Alb-PepI, PepGAT, and PepKAA to zebrafish embryos. (A) Survival rate (%) of zebrafish embryos and larvae exposed to 1 mg mL of each synthetic peptide and control (E3 medium) samples after 96 h. (B−F) Zebrafish larvae exposed to, respectively, control (E3 medium), *Mo*-CBP$_3$-PepII, *Rc*Alb-PepI, PepGAT, and PepKAA 1 mg mL^{-1} for 96 h. All organisms presented normal development even exposed to peptides. Data are shown as mean ± standard deviation of three independent experiments.

interaction was supported by hydrogen bonds among amino acid residues of S^{D614G} Lys^{386}, Asp^{389}, Asn^{544}, Arg^{567}, Asn^{969}, Ile^{973} and Arg^{983}, with respective distances of 2.8, 2.7, 2.6, 2.4, 3.3, 2.8, and 2.4 Å (Figure 3B). *Mo*-CBP$_3$-PepII also exhibited hydrophobic interactions with the residues Leu^{518}, Ser^{974}, Leu^{517}, Thr^{430}, Phe^{565}, His^{519}, Cys^{391}, Ala^{522}, Gly^{545}, Leu^{546}, Ser^{982}, and Leu^{390} of S^{D614G} (Figure S2A).

*Rc*Alb-PepI had a LBEI value with S^{D614G} of −646.9 kJ·mol^{-1}, supported by six hydrogen bonds and 14 hydrophobic interactions with S^{D614G}. The hydrogen bonds were with the residues Asp^{428}, Leu^{546}, Thr^{547}, and Asp^{979}, with distances of 2.6, 2.6, 2.6, 2.7, 2.8, and 3.0 Å (Figure 3D). The hydrophobic interactions were formed by Ile^{973}, Thr^{430}, Ser^{974}, Leu^{518}, Ser^{982}, His^{519}, Arg^{983}, Leu^{517}, Gln^{564}, Phe^{565}, Gly^{545}, Leu^{390}, Cys^{391}, and Asn^{544} of S^{D614G} (Figure S2B).

The LBEI between PepGAT and S^{D614G} was −605.5 kJ·mol^{-1}. Ten hydrogen bonds between the PepGAT and the amino acid residues Thr^{430}, Asp^{979}, Asp^{428}, Arg^{567}, Ser^{975}, and Ala^{520} of S^{D614G} and 10 hydrophobic interactions between Arg^{983}, Ile^{973}, Cys^{391}, Leu^{390}, Leu^{518}, Leu^{517}, Ser^{974}, Asp40, Phe^{565}, Val^{42}, and His^{519} supported the PepGAT-S^{D614G} complex (Figures 3F and S2C).

PepKAA (LBEI, −779.4 kJ·mol^{-1}) interacted with S^{D614G} by hydrogen bonds with the amino acid residues Asp^{198}, Glu^{516}, Arg^{567}, Asp^{571}, Thr^{547}, Thr^{573}, and Asn^{544}, with distances of 2.7,

2.6, 2.8, 2.9, 3.1, 2.7, and 2.7 Å, respectively (Figure 3H). PepKAA also exhibited hydrophobic interactions with Tyr^{200}, Leu^{517}, Leu^{518}, Ser^{974}, Asn^{969}, His^{519}, Arg^{983}, Ser^{975}, Val^{976}, Phe^{565}, Ala^{522}, Leu^{390}, Gly^{545}, Leu^{546}, and Cys^{391} of S^{D614G} with PepKAA (Figure S2D).

To find possible clinical applications of peptides, their toxicity to human cells was assessed (Figure 4). The MTT assay revealed that the peptides were not toxic to the human cells tested. All cells treated with peptides presented 100% viability (Figure S3). Additionally, we performed two other experiments to evaluate the peptides' safety on human cells. In the first experiment, we tested whether the peptides would induce DNA damage (Figure 4A−C) to three cell lines: L929 fibroblast cells from mice and two human lines—human fetal lung fibroblast (MRC-5 line) and human keratinocytes (HaCaT line). At a concentration of 1 mg mL^{-1}, the comet assay revealed that all peptides caused no damage to DNA (Figure 4A−C). In contrast, in the positive control for DNA damage, the methyl methanesulfonate (MMS) (4 × 10^{-5} M) agent caused severe damages to the cells' DNA.

The second experiment analyzed whether peptides can induce apoptosis in the same cell line at a concentration of 1 mg mL^{-1} (Figure 4D−F). At that concentration of peptides, the treated cells presented no characteristics of apoptosis (Figure 4D,E). In contrast, cells treated with 4 × 10^{-5} M presented all aspects of apoptosis, such as small cell volume, fragmented nucleus,

peripheral condensation of chromatin, and apoptotic bodies (Figure 4D,E).

Toxicity of Peptides to Zebrafish Embryos. To assess in depth the safety of peptides, the toxicology to zebrafish embryos was evaluated (Figure 5). The survival rates of zebrafish larvae and embryos after exposure to 1 mg mL^{-1} of the peptides for 96 h were ≥90% (Figure 5A). After 96 h of treatment, morphological analysis revealed no alterations (nonlethal effects) in the embryos exposed to the control (Figure 5B) and peptides (Figure 5C−F). The embryo coagulation rates were ≤20% in the control and peptide-tested embryos (Figure 5B−F). This is an expected and spontaneous natural process that happens in zebrafish embryos, leading to a mortality rate of 5−25%.

■ DISCUSSION

At the beginning of the current outbreak, it was thought that vaccines would be the only way to fight back SARS-CoV-2. Thus, an unprecedented collaboration worldwide led to the development of vaccines in record times.[14,15] However, together with the beginning of vaccination came SARS-CoV-2 variants not affected or weakly affected by the immune response produced by vaccines.[16] The first vaccines applied brought widespread hope that vaccination would end the pandemic. However, what nobody expected was the emergence of many SARS-CoV-2 variants due to mutations, reducing the vaccines' efficiency. For example, a mutation in the RBD of the S protein at position E484 reduced the SARS-CoV-2 neutralization by monoclonal antibodies and convalescent sera.[16] Thus far, there are more than 3.5 billion people vaccinated worldwide.[17,18] Even though this number has been reached in short a time, the WHO and American Centers for Disease Control (CDC) have reported that some fully vaccinated people have still been infected by SARS-CoV-2. Thus, they are advising even fully vaccinated people to continue using masks to prevent infection by variants.[19−21]

The emergence of these SARS-CoV-2 variants and the existence of people at greater risk such as immunosuppressed patients and those who cannot be vaccinated, such as young children, makes it important to develop drug/treatments specific for SARS-CoV-2 that can abolish or alleviate the symptoms of infected patients. To find such drugs quickly, many groups have examined drug repositioning, so far without success. Many antiviral drugs such as arbidol, an anti-influenza drug targeting the S protein, and galidesivir, remdesivir, tenofovir, sofosbuvir, and ribavirin, which target the RdRp, have been submitted to in silico assays for use against SARS-CoV-2.[22,23] Of these drugs, the studies with arbidol have gone the furthest. Wang et al.[24] reported that at a concentration of 1.9 mg mL^{-1}, arbidol achieved EC$_{50}$ to SARS-CoV-2. They also suggested a dosage of 200 mg 3 times/day or even higher to alleviate COVID-19 symptoms. In another study, Yang et al.[25] revealed that in a group of 82 health professionals treated prophylactically with arbidol, 48 people (58.5%) were infected by SARS-CoV-2 and hospitalized and 34 (41.5%) developed mild symptoms of COVID-19. Altogether, these results suggest that arbidol is not very effective, so new drugs need to be developed. Nevertheless, it was approved for the treatment of patients with COVID-19 by the National Medical Products Administration of China.

In our previous study,[8] it was shown that *Mo*-CBP$_3$-PepII and PepKAA strongly bind to the S protein, leading to changes in three-dimensional (3D) conformational structures and misplaced interactions with the ACE2 receptor.[8] Here, we have shown that all four peptides interact with S^{D614G}, altering its conformational structure (Figures 3 and S2). Thus, it is feasible to suggest that these peptides block the entrance of SARS-CoV-2 in cells by interacting with the S protein. In silico studies predicted that PepKAA, by strongly interacting with both S[8] and S^{D614G} (Figures 3 and S2) and changing their 3D, could be the best peptide to block SARS-CoV-2 entrance in cells. Those results were confirmed by in vitro experiments (Figures 1 and 2). Based on all our results, PepKAA is the best peptide to inhibit SARS-CoV-2 S^{D614G} in cells, by reducing the virus plaque number by 60% at the lowest concentration (0.15 mg mL^{-1}). This study is very important because the active concentration of PepKAA is 47.5-fold lower than that of arbidol, the most widely studied drug against SARS-CoV-2.[24,25]

Studying the repositioning of other antiviral drugs, Sacramento et al.[26] employed a combination of daclatasvir and sofosbuvir, two anti-HCV drugs (Hepatitis C virus), against SARS-CoV-2 at concentrations higher than that employed to treat HCV. Wang et al.[27] reported that other antiviral drugs such as penciclovir, ribavirin, faviparin, and remdesivir had EC$_{50}$ values in vitro against SARS-CoV-2, respectively, of 0.1, 0.98, 0.062, and 0.062 mg mL^{-1}. These results show that PepKAA is a good candidate to be used as a source to develop a new drug against SARS-CoV-2. Of these drugs, only arbidol and remdesivir have been investigated beyond in vitro tests. However, as reported above, arbidol was not very efficient.[25] Although approved by the FDA (U.S. Food and Drug Administration), the results of remdesivir in clinical trials presented no significant differences between the placebo and the drug-treated group of patients.[28] Therefore, the search for new drugs to block SARS-CoV-2 is still necessary.

Based on our data, of all peptides tested here, PepKAA is likely the best one to neutralize SARS-CoV-2 S^{D614G}, by preventing cell infection (Figures 1 and 2). However, other peptides are also promising to inhibit SARS-CoV-2, such as *RcAlb*-PepI and PepGAT (Figures 1 and 2). Here, data from in vitro (Figures 1 and 2) and in silico tests (Figures 3 and S2) of PepKAA are in harmony and may explain its high efficiency against SARS-CoV-2. Souza et al.[8] reported that PepKAA interacted with the S protein with an LBEI of −715.6 kJ·mol^{-1}, by inducing a conformational change in the S protein. The authors showed that PepKAA led to the incorrect interaction of S protein and ACE2 receptor, suggesting that the formation of the PepKAA-S protein complex inhibits the entrance of SARS-CoV-2 in cells.[8]

In another study, Amaral et al.[9] predicted that PepKAA has a strong interaction with M^{pro} of SARS-CoV-2, leading to conformational changes and reduction of the active site. These findings suggest that PepKAA reduced the M^{pro} activity. M^{pro} is vital for SARS-CoV-2 replication because SARS-CoV-2 is an RNA virus producing a polyprotein that is cleaved by Mpro, releasing SARS-CoV-2 proteins.[4,9] Here, the molecular docking study predicted that PepKKA has the highest LBEI for S^{D614G} compared to other peptides (Figure 3). The LBEI of PepKAA to S^{D614G} was −779.4 kJ·mol^{-1}, which is very similar to that presented for the wild-type S protein, −715.6 kJ·mol^{-1}.[8] PepKAA did not interact close to the G614 mutation, but the interaction was still important to induce conformational changes in the S^{D614G} protein, which could induce the wrong interaction with the ACE2 receptor.

Here, in all assays, PepKAA was first incubated with SARS-CoV-2 for 30 min to interact with the S^{D614G} protein before infecting cells. Interestingly, even when the virus, peptides, and cells were incubated at the same time, PepKAA could not

prevent cell infection by SARS-CoV-2 (data not shown). These results strongly suggest that the mechanism behind PepKAA's anti-SARS-CoV-2 activity is by interacting with S^{D614G}, inducing conformational changes (as revealed by docking), wrongly interacting with the ACE2 receptor,[8] and thus inhibiting SARS-CoV-2 from invading the cell. Also, it is feasible to suggest that by a so-far-unclear mechanism, PepKAA inhibits M^{pro} activity, which also prevents SARS-CoV-2 replication and infection. We hypothesize this because PepKAA is a membrane-penetrating peptide[12] and SARS-CoV-2 has a lipid envelope.[4] Thus, PepKAA could also target the SARS-CoV-2 membrane, inactivating it. In that case, PepKAA could inhibit SARS-CoV-2 by different mechanisms.

Recently, other synthetic peptides have been tested against SARS-CoV-2.[29−31] Curreli et al.[29] have analyzed the interaction of RBD from SARS-CoV-2 with human ACE2. From this analysis, the authors designed and synthesized four peptides. Among those, the synthetic peptide NYBSP-4 presented an IC_{50} of 1.97 μM against SARS-CoV-2. This result is better than that showed for PepKAA, which reached the same inhibition at a concentration of 12.1 μM. However, compared to results reported by Larue et al.,[30] PepKAA seems to be more effective. Larue et al.[30] reported that synthetic peptides SAP1, SAP2, and SAP6 derived from human ACE2 receptor displayed an IC_{50} toward SARS-CoV-2 at concentrations of, 2.39, 3.72, and 1.90 mM, respectively, which are much higher than the concentration of 12.1 μM presented by PepKAA. In another study, Han et al.[31] reported that the peptide GK-7, also derived from human ACE2, presented an IC_{50} toward SARS-CoV-2 at a concentration of 3.8 μM, which is lower than the concentration presented by PepKAA (12.1 μM). It is important to notice that all studies performed the antiviral assay using a pseudovirus expressing the S protein.[29−31] In our case, we employed the entire natural virus isolated from a patient with full fitness to infect cells in the assay, which is closer than what occurs during infection. This could be an explanation for the elevated concentration required for PepKAA to reach the same concentration presented by other peptides. This result still highlights the efficiency and the potential of PepKAA toward SARS-CoV-2.

One important feature of a candidate drug is safety. New drugs must cause no or very low side effects. In the case of arbidol and remdesivir, this is not true. Both have considerable side effects.[32−34] Yet despite this, they were approved for treatment given the emergency faced by the population from the SARS-CoV-2 outbreak. Arbidol was hastily approved to treat COVID-19 in China, even without satisfactory results. The use of arbidol was associated in rats with loss of body weight, loss of organ weight (mainly liver), and piloerection in females.[34] In the case of remdesivir, the side effects reported were from patients with COVID-19 using the drug to treat symptoms. The side effects reported were increased nausea, diarrhea, vomiting, gastroparesis, atrial fibrillation, cardiac arrest, and acute kidney injury.[35] It is important to state that we are not criticizing or judging the use of these drugs. Because they were approved, they should be used. However, it is also urgently necessary to seek a new type of drug that has lower or no toxic effects.

In this context, PepKAA is a strong candidate. PepKAA was meticulously designed to prevent any kind of toxic effect.[12] Indeed, the bioinformatics analysis revealed no allergic or toxic potential. The hemolytic analysis revealed only 5% chance to cause hemolysis on erythrocytes. However, the in vitro tests against erythrocytes revealed no hemolysis. PepKAA did not present any toxicity to Vero cells.[12] Here, looking toward clinical trials with PepKAA and/or other peptides, we performed additional toxicity tests. Not only PepKAA but also all synthetic peptides presented no genotoxicity or pro-apoptotic effects on human cells L929, MRC-5, and HaCaT (Figure 4) at a concentration of 1 mg mL^{-1}, which is threefold higher than the highest concentration tested (Figure 1). To shed more light on the toxicity of peptides, we employed an important tool for drug development: testing by the zebrafish model.[36] At a concentration of 1 mg mL, none of the peptides presented toxicity to zebrafish larvae and embryos (Figure 5). That concentration (1 mg mL^{-1}) is 25-fold higher than the EC50 value of PepKAA against SARS-CoV-2. In this assay, we used 20 zebrafish embryos, and the embryos incubated with the peptides had a survival of ≥95%. In the case of PepKAA, the survival was 100% (Figure 5A), and no damage was found in the zebrafish (Figure 5C−H). Altogether, the results of efficacy against SARS-CoV-2 and safety indicated PepKAA as a potential substance for testing the development of new drugs against SARS-CoV-2.

PepKAA is a synthetic peptide. One question always arises when working with synthetic peptides: are they cost-effective for commercial use? During the 1990s, the employment of synthetic peptides was impossible given the high cost of chemicals used in the synthesis combined with a very low yield. However, new technologies allowing the recovery and recycling of solvents used during synthesis have made it feasible to produce with a kilogram scale, leading to a dramatic reduction in the cost of peptide synthesis.[37] The synthetic peptide Fuzeon is an example. It is a peptide used in the treatment of HIV requiring kilogram-scale production (≥100 kg), which is possible due to these new technologies.[38] In 2018, the FDA approved a glucagon-like synthetic peptide, Rybelsus, used in the treatment of type II diabetes.[39] Therefore, if the pharmaceutical industry demonstrates interest, the application of synthetic peptides is surely practicable. Based on the potential of our peptides, we filed a patent application in Brazil with the National Industrial Property Institute, under number BR 10 2020 023728 4.

■ CONCLUSIONS

Here, all synthetic peptides were active against SARS-CoV-2 to some extent. The ability to interact with S^{D614G} provided a clue about how peptides act to inhibit SARS-CoV-2. PepKAA was the most prominent peptide to inhibit SARS-CoV-2 while showing no toxicity to human cells and zebrafish embryos. PepKAA thus has a higher potential to develop new anti-SARS-CoV-2 drugs that are effective without adverse effects.

■ METHODOLOGY

Ethical Statement. This experiment conducted with a human patient in this study was approved by the Research Ethics Committee involving human beings on the use of humans in experiments of the Federal Univerisity of Ceará, with authorization documented by protocol no. 4.029.490. All experiments with SARS-CoV-2 were done in accordance with relevant guidelines and regulations. Additionally, the informed consent was obtained from all participants and/or their legal guardian(s).

The experiments conducted with zebrafish in this study were approved by the Ethics Committee in the Use of Animals of the Federal University of Paraíba, with authorization documented by protocol no. 4460140920. In addition to this, animal use methods were carried out in compliance with the ARRIVE

guidelines and in accordance with relevant guidelines and regulations.

Sample Collection. The clinical sample was collected from a patient with positive real-time (RT)-qPCR result and presenting symptoms of SARS-CoV-2 infection. A nasopharyngeal swab was used to collect the sample, and the sample was placed into a 3 mL tube containing a viral transportation solution, as described by Holshue et al.[40] All experiments were carried out in the biosafety level 3 facility (NB-3) of the Laboratory of Emerging and Reemerging Pathogens of the Federal University of Ceará (Fortaleza, Brazil).

Viral Isolation and Titration. The SARS-CoV-2 isolation was performed following the protocol described by Harcourt et al.[41] with modifications. Vero E6 cells (ATCC number CCL-81) were cultured in a Leibovitz medium (L-15) supplemented with 2% heat-inactivated fetal bovine serum (FBS) and 1% penicillin/streptomycin solution (GIBCO). The frozen sample was thawed and passed through a 22 μm syringe filter. The viral isolation was carried out in a 96-well plate containing a Vero cell monolayer with 90−100% confluence. Then, 50 μL of the L-15 medium without FBS was added to 100 μL of the clinical material. Then, the plate was incubated for 2 h at 37 °C, with shaking every 15 min to facilitate the infection of cells by the virus. After the incubation, the medium was removed and added to all wells containing 100 μL of L-15 with 2% FCS and 1% penicillin/streptomycin, incubated at 37 °C and observed daily for the presence of cytopathic effects. The material in the wells in which cytopathic effects were observed was submitted to confirmatory testing using RT reverse transcription PCR. The supernatant from the infected Vero cells was collected, placed into cryotubes, and stored at −80 °C. The virus titration was done following the method described by Mendoza et al.[42]

RT PCR and Sequencing. SARS-CoV-2 RNA was extracted using the QIAamp Viral RNA kit (Qiagen) following the manufacturer's instructions for SARS-CoV-2 detection using a one-step procedure. For RT PCR (qPCR), the CDC 2019-nCoV qPCR diagnostic panel was followed, using specific primers to confirm the presence of SARS-CoV-2 in all cell cultures. In this kit, the primer−probe mixes target two regions of the nucleocapsid gene (N1 and N2) as well as the human endogenous control (RNase P gene), a control for sample integrity.

Thereafter, a specific RBD region of the spike gene was amplified from the cDNA sample using the paired primers (F-AATCTATCAGGCCGGTAGCAC and R-CACCAATGGG-TATGTCACACT) and Platinum Taq DNA Polymerase High-Fidelity kit (Invitrogen). The PCR product was analyzed by electrophoresis through 1.5% agarose gel and purified using the PureLink PCR Purification Kit (Thermo Fisher). The purified product was sequenced using the BigDye Terminator v1.1 Cycle Sequencing Kit (Thermo Fisher) according to the manufacturer's instructions. The basic local alignment search tool software was used for the computer analysis of sequence data with the reference sequence from Wuhan, China (NC_045512.2).

By amplifying the N gene as a target, we confirmed the presence of SARS-CoV-2. After the confirmation, we performed partial sequencing of the RBD region of the S protein, revealing the presence of mutation A23231G, which corresponds to the D614G mutation in the spike protein (S^{D614G}).

Anti-SARS-CoV-2 Activity of Peptides by the MTT Assay. The peptides were diluted to a concentration ranging from 0 to 2.5 mg mL^{-1} in the L-15 medium (Cultilab, Brazil)

without fetal serum and filtered through 22 μm filters. The peptides were mixed with an equal volume of viral solution and incubated for 30 min at 37 °C. After incubation, the mixture from each peptide dilution and a multiplicity of infection (MOI) of 1.85 were added in triplicate to a 96-well plate containing 2.5 × 10^5 cells per well. After 2 h of incubation at 37 °C, the virus-containing mixtures were removed from the wells and replaced by fresh L-15 medium containing 2% FBS and 1% antibiotic. The plate was incubated for 4 days at 37 °C. The negative control wells received only the culture medium, and the positive control wells received the virus. After this period, the medium was removed, and 50 μL of 5 mg mL^{-1} MTT (3-4,5-dimethylthiazol-2-yl)-25 diphenyl tetrazolium bromide (Life Technologies, USA) was added. The plate remained for 4 h at 37 °C, after which the solution was removed, and the formazan crystals were diluted with 50 μL DMSO. The plate was read at 540 nm, and the percentage of protection (PP) was calculated by the following formula: PP = [(AB)/(CB) × 100], where A, B, and C indicate the absorbance of the peptide, virus, and control cells, respectively.[43]

Plaque Reduction Neutralization Tests. The neutralization assay was performed as described by Muruato et al.[44] Vero E6 cells (6 × 10^5 per well) were seeded in 12-well plates and left at rest overnight. Then, SARS-CoV-2 samples at an MOI of 1.85 were incubated with the peptides at concentrations of 0.15 and 0.30 mg mL^{-1} at 37 °C for 1 h. The virus−peptide mixture was added in triplicate to pre-seeded Vero E6 cells at 90−100% confluence. After 2 h of incubation at 37 °C, 1 mL of the overlay containing 1.5% carboxymethylcellulose in L-15 containing 2% FBS and 1% penicillin/streptomycin antibiotics (GIBCO) was added to the infected cells. After 3 days of incubation, 1 mL of 3.65% formaldehyde in phosphate-buffered saline (PBS) was added to the overlay-covered cells. After fixation for 1 h, the overlay was removed, and the contents of the cells were stained with 0.5% crystal violet. The plates were washed with water to remove excess dye, photographed, and submitted for counting using the ImageJ program. Percentage plaque reduction was calculated using the following formula: [(sample × 100)/positive control] −100.

Molecular Docking Analysis. The crystallographic data of the mutant (D614G) SARS-CoV-2 protein S was obtained from the Protein Data Bank, with accession number PDB ID: 7DX1. The 3D structures of peptides *Mo*-CBP$_3$-PepII, *Rc*Alb-PepI, PepGAT, and PepKAA were predicted using the PEP-FOLD 3.5 software.[45] The protein and peptide structures were determined and the protonation states were adjusted using the ProteinPrepare software.[46]

To carry out molecular docking between the peptides and the mutated protein S of SARS-CoV-2, we used the ClusPro 2.0 server,[47] which showed the best results in the CAPRI challenge.[48] The results were analyzed using the number of members in each cluster and the lowest energies calculated through the Balanced software method, which considers the energies obtained from electrostatic and hydrophobic interactions.

To analyze the interactions between the peptides and the mutated S protein, the software LigPlot$^+$ v. 2.2.4 was used.[49] The preparation of figures and measurement of the variation in rmsd were performed with the Pymol software.

Assessment of Cytotoxicity. The cytotoxicity was quantified by the ability of live cells to reduce the yellow dye 3-(4,5-dimethyl-2-thiozolyl)-2,5-diphenyl-2H-tetrazolium bromide (MTT) to formazan.[50] Cytotoxicity was checked against

L929 (murine fibroblasts, ATCC number CCL-1), MRC-5 (human lung fibroblasts, ATCC number CCL-171), and HaCat (human keratinocytes), provided by the Rio de Janeiro Cell Bank (BCRJ, Brazil). All cell lines were washed and resuspended in the DMEM medium supplemented with 10% FBS, 2 mM of glutamine, 100 U/mL of penicillin, and 100 μg/mL of streptomycin, at 37 °C under 5% CO_2. For the experiments, cells were plated in 96-well plates (0.1×10^6 cells/mL for HaCat cells and 0.1×10^4 cells/mL for L929 and MRC-5 cell lines). After 24 h, the tested peptides (1 mg mL^{-1} in the culture medium) were added to each well, and the cells were incubated for 72 h. MMS (4×10^{-5} M) was used as the positive control. Thereafter, the plates were centrifuged, and the medium was replaced with a fresh medium (150 μL) containing 0.5 mg mL of MTT. Three hours later, the MTT formazan product was dissolved in 150 μL DMSO, and the absorbance was measured using a multiplate reader (Spectra Count, Packard, Ontario, Canada). Drug effect was quantified as the percentage of control absorbance of the reduced dye at 595 nm.

Comet Assay. For this assay, the concentration of peptides was 1 mg mL^{-1}. DMSO−NaCl was the negative control for damage, and MMS (4×10^{-5} M) was used as the positive control for DNA damage. The standard alkaline comet assay (single-cell gel electrophoresis) was performed as previously described.[51] After treatment (24 h), cells were washed with ice-cold PBS, trypsinized, and resuspended in the complete medium. Then, 20 μL of cell suspension (0.7×10^5 cells/mL) was dissolved in 0.75% low-melting-point agarose and immediately spread onto a glass microscope slide pre-coated with a layer of 1% agarose with a normal melting point. The agarose was allowed to set at 4 °C for 5 min. Slides were incubated in an ice-cold lysis solution (2.5 M NaCl, 0.01 M Tris, 0.1 M EDTA, 1% Triton X-100, and 10% DMSO, pH 10.0) at 4 °C for at least 1 h to remove cell membranes, leaving DNA as "nucleoids".

After that, the slides were placed in a horizontal electrophoresis unit and incubated with a fresh buffer solution (0.3 M NaOH, 0.001 M EDTA, pH 13.0) at 4 °C for 20 min to allow DNA unwinding and the expression of alkali-labile sites. Electrophoresis was conducted for 20 min at 25 V (94 V/cm). All the above steps were performed in the dark to prevent additional DNA damage. Slides were neutralized (0.4 M Tris, pH 7.5) and stained using 20 μg mL ethidium bromide (EB). One hundred and fifty cells (50 cells from each of the three replicate slides for each treatment) were selected, coded, and blindly analyzed for DNA migration. These cells were visually scored according to the tail length into five classes: (1) class 0: undamaged, without a tail; (2) class 1: with a tail shorter than the diameter of the head nucleus; (3) class 2: with a tail length 1−2× the diameter of the head; (4) class 3: with a tail longer than 2× the diameter of the head; and (5) class 4: comets with no heads. The damage index (DI) value was assigned to each sample. DI is an arbitrary score based on the number of cells in the different damage classes, which are visually scored by measuring the DNA migration length and the amount of DNA in the tail. DI ranges from 0 (no tail: 100 cells × 0) to 400 (with maximum migration: 100 cells × 4).[52]

Morphological Characterization of Apoptotic PBLs. For this assay, the concentration of peptides was 1 mg mL^{-1}. DMSO−NaCl was the negative control for damage, and MMS (4×10^{-5} M) was used as the positive control for DNA damage. The peptide and control solutions were incubated as described above. Then, cells with morphological characteristics of apoptosis (i.e., small cell volume, peripheral condensation of

chromatin, fragmented nucleus, and apoptotic bodies) were determined after each treatment (24 h) by the acridine orange (AO)/EB staining assay: 25 μL of the cell suspension was mixed with 1 μL of the staining solution (100 μg/mL AO + 100 μg/mL EB in PBS) and spread on a slide, where 300 cells were counted per data point. The percentage of apoptotic cells was then calculated.[53]

Zebrafish Toxicity. *Zebrafish Embryos.* Zebrafish embryos (AB wild-type strain) with approximately 1 HPF (hour post-fertilization) were provided by the Production Unit for Alternative Model Organisms (UniPOM), Federal University of Paraíba, João Pessoa, Brazil. The parents were maintained in a recirculation system with regular monitoring of water quality parameters (pH, ammonia, and nitrite levels) in a room with controlled temperature (26 ± 1 °C) and photoperiod (14:10 light/dark cycle). Fish were fed daily with commercial feed (Color Bits Tetra, Melle, Germany) and freeze-dried spirulina (Fazenda Tamanduá, Patos, Brazil) and were monitored for abnormal behavior or disease development.

Before the experiment, adult zebrafish (male-to-female ratio of 2:1) were transferred to a 7 L spawning tank with a bottom mesh and a quick-opening valve for embryo collection. Embryos were collected on the day of the experiment and cultured in an adapted embryonic medium E3 (5.0 mM NaCl, 0.17 mM KCl, 0.33 mM CaCl, and 0.33 mM MgSO4) containing 0.005% methylene blue. Only spawning samples with a fertilization rate ≥90% were used. Viable embryos (normal cleavage pattern and without morphological changes) were selected under an inverted light microscope (Televal 31, Zeiss, Germany), at 50× magnification.

Acute Toxicity Test. The fish embryo acute toxicity test was independently conducted with four peptides according to the OECD Guideline number 236[54] adapted for 96-well plates by Muniz et al.[55] Zebrafish embryos with up to 3 hpf were exposed to 1 mg mL^{-1} of each sample. For each test and control sample, 20 wells were filled with 0.3 mL of solution and 1 embryo.

Additionally, 20 embryos were exposed only to the E3 medium (the solvent control). Lethal and non-lethal effects were observed daily for 96 h. Embryos showing lethality endpoints (coagulation, no formation of somites, no detachment of tail, or absence of heartbeat) were considered dead. This number was used to determine the survival percentage (number of live organisms/total number of organisms × 100) per tested sample. The exposures were under static conditions (without the renovation of the exposure solution). Observations were performed with a stereomicroscope (Olympus SZX7, Japan) at 56× magnification and photographed (Moticam 5+, China). After 96 h, surviving larvae were euthanized with eugenol and properly discarded.

Statistical Analysis. The assays were performed in three independent experiments. The statistics were expressed as the mean ± standard deviation. The data were submitted to ANOVA followed by the Tukey test, using GraphPad Prisma 5.01, with a significance of $p < 0.05$.

■ ASSOCIATED CONTENT

Ⓢ Supporting Information

The Supporting Information is available free of charge at https://pubs.acs.org/doi/10.1021/acsomega.2c02203.

Clustal alignment of the SARS-CoV-2 nucleotide sequence of the receptor-binding domain from S protein; two-dimensional demonstration of the interaction

between peptides and mutated protein SD[614G]; and assessment of the toxicity of Mo-CBP3-PepII, RcAlb-PepI, PepGAT, and PepKAA to human cell lines by cell viability assay (PDF)

■ AUTHOR INFORMATION

Corresponding Author

Pedro F.N. Souza − *Department of Biochemistry and Molecular Biology, Federal University of Ceará, Fortaleza, Ceará 60020-181, Brazil; Drug Research and Development Center, Department of Physiology and Pharmacology, Federal University of Ceará, Fortaleza, Ceará 60020-181, Brazil;* ● orcid.org/0000-0003-2524-4434; Email: pedrofilhobio@gmail.com

Authors

Maurício F. vanTilburg − *Biotechnology and Molecular Biology Laboratory, Renorbio, State University of Ceará, Fortaleza, Ceará 60020-181, Brazil*

Felipe P. Mesquita − *Drug Research and Development Center, Department of Physiology and Pharmacology, Federal University of Ceará, Fortaleza, Ceará 60020-181, Brazil*

Jackson L. Amaral − *Department of Biochemistry and Molecular Biology, Federal University of Ceará, Fortaleza, Ceará 60020-181, Brazil*

Luina B. Lima − *Drug Research and Development Center, Department of Physiology and Pharmacology, Federal University of Ceará, Fortaleza, Ceará 60020-181, Brazil*

Raquel C. Montenegro − *Drug Research and Development Center, Department of Physiology and Pharmacology, Federal University of Ceará, Fortaleza, Ceará 60020-181, Brazil*

Francisco E.S. Lopes − *Department of Biochemistry and Molecular Biology, Federal University of Ceará, Fortaleza, Ceará 60020-181, Brazil*

Rafael X. Martins − *Laboratory for Risk Assessment of Novel Technologies (LabRisk), Department of Molecular Biology, Federal University of Paraiba, João Pessoa, Paraíba 58051-900, Brazil*

Leonardo Vieira − *Laboratory for Risk Assessment of Novel Technologies (LabRisk), Department of Molecular Biology, Federal University of Paraiba, João Pessoa, Paraíba 58051-900, Brazil*

Davi F. Farias − *Laboratory for Risk Assessment of Novel Technologies (LabRisk), Department of Molecular Biology, Federal University of Paraiba, João Pessoa, Paraíba 58051-900, Brazil*

Ana C.O. Monteiro-Moreira − *School of Pharmacy, University of Fortaleza, Fortaleza, Ceará 60811-690, Brazil*

Cleverson D.T. Freitas − *Department of Biochemistry and Molecular Biology, Federal University of Ceará, Fortaleza, Ceará 60020-181, Brazil*

Arnaldo S. Bezerra − *Biotechnology and Molecular Biology Laboratory, Renorbio, State University of Ceará, Fortaleza, Ceará 60020-181, Brazil*

Maria I.F. Guedes − *Biotechnology and Molecular Biology Laboratory, Renorbio, State University of Ceará, Fortaleza, Ceará 60020-181, Brazil*

Débora S.C.M. Castelo-Branco − *Department of Pathology and Legal Medicine, Federal University of Ceará, Fortaleza, Ceará 60020-181, Brazil*

Jose T.A. Oliveira − *Department of Biochemistry and Molecular Biology, Federal University of Ceará, Fortaleza, Ceará 60020-181, Brazil;* ● orcid.org/0000-0003-1207-1140

Complete contact information is available at:
https://pubs.acs.org/10.1021/acsomega.2c02203

Author Contributions

Conceptualization: P.F.N.S., M.F.T., F.P.M. Data curation: P.F.N.S., M.F.T., F.P.M., J.L.A., L.B.L., R.X.M., L.V., D.F.F., A.S.B. Formal analysis: P.F.N.S., D.F.F., M.F.T., F.P.M., J.L.A., Funding acquisition: R.C.M., D.F.F., A.C.O.M.M., C.D.T.F., M.I.F.G., D.S.C.M.C.-B. J.T.A.O. Methodology: P.F.N.S., M.F.T., F.P.M., J.L.A., A.S.B. Resources: P.F.N.S., R.C.M., D.F.F., A.C.O.M.M., C.D.T.F., M.I.F.G., D.S.C.M.C.-B. J.T.A.O. Supervision: P.F.N.S., and F.P.M. Writing original draft: P.F.N.S., and F.P.M. Writing, review, and editing: F.P.M., M.F.T., F.P.M., D.S.C.M.C.-B., P.F.N.S.

Notes

The authors declare no competing financial interest.

■ ACKNOWLEDGMENTS

■ REFERENCES

(1) WHO Coronavirus (COVID-19) Dashboard | WHO Coronavirus (COVID-19) Dashboard With Vaccination Data https://covid19.who.int/ (accessed Jul 9, 2021).

(2) Wang, C.; Horby, P. W.; Hayden, F. G.; Gao, G. F. A Novel Coronavirus Outbreak of Global Health Concern. *Lancet* **2020**, *395*, 470−473.

(3) Zhang, T.; Wu, Q.; Zhang, Z. Probable Pangolin Origin of SARS-CoV-2 Associated with the COVID-19 Outbreak. *Curr. Biol.* **2020**, *30*, 1346−1351.

(4) Souza, P. F. N.; Mesquita, F. P.; Amaral, J. L.; Landim, P. G. C.; Lima, K. R. P.; Costa, M. B.; Farias, I. R.; Lima, L. B.; Montenegro, R. C. The Human Pandemic Coronaviruses on the Show: The Spike Glycoprotein as the Main Actor in the Coronaviruses Play. *Int. J. Biol. Macromol.* **2021**, *179*, 1−19.

(5) Lazarus, J. V.; Ratzan, S. C.; Gostin, L. O.; Larson, H. J.; Rabin, K.; Kimball, S. A Global Survey of Potential Acceptance of a COVID-19 Vaccine. *Nat. Med.* **2021**, *27*, 225−228.

(6) Alam, I.; Radovanovic, A.; Incitti, R.; Kamau, A. A.; Alarawi, M.; Azhar, E. I.; Gojobori, T. CovMT: An Interactive SARS-CoV-2 Mutation Tracker, with a Focus on Critical Variants. *Lancet Infect. Dis.* **2021**, *21*, 602.

(7) Serafin, M. B.; Bottega, A.; Foletto, V. S. Drug Repositioning Is an Alternative for the Treatment of Coronavirus COVID-19. *Int. J. Antimicrob. Agents* **2020**, *55*, 105969.

(8) Souza, P. F. N.; Lopes, F. E. S.; Amaral, J. L.; Freitas, C. D. T.; Oliveira, J. T. A. A Molecular Docking Study Revealed That Synthetic Peptides Induced Conformational Changes in the Structure of SARS-CoV-2 Spike Glycoprotein, Disrupting the Interaction with Human ACE2 Receptor. *Int. J. Biol. Macromol.* **2020**, *164*, 66−76.

(9) Amaral, J. L.; Oliveira, J. T. A; Lopes, F. E. S.; Freitas, C. D. T.; Freire, V. N.; Abreu, L. V.; Souza, P. F. N. Quantum Biochemistry,

Molecular Docking, and Dynamics Simulation Revealed Synthetic Peptides Induced Conformational Changes Affecting the Topology of the Catalytic Site of SARS-CoV-2 Main Protease. *J. Biomol. Struct. Dyn.* **2021**, 1.

(10) Dias, L. P.; Souza, P. F. N.; Oliveira, J. T. A.; Vasconcelos, I. M.; Araújo, N. M. S.; Tilburg, M. F. V.; Guedes, M. I. F.; Carneiro, R. F.; Lopes, J. L. S.; Sousa, D. O. B. RcAlb-PepII, a Synthetic Small Peptide Bioinspired in the 2S Albumin from the Seed Cake of Ricinus Communis, Is a Potent Antimicrobial Agent against Klebsiella Pneumoniae and Candida Parapsilosis. *Biochim. Biophys. Acta Biomembr.* **2020**, *1862*, 183092.

(11) Oliveira, J. T. A.; Souza, P. F. N.; Vasconcelos, I. M.; Dias, L. P.; Martins, T. F.; Van Tilburg, M. F.; Guedes, M. I. F.; Sousa, D. O. B. Mo-CBP3-PepI, Mo-CBP3-PepII, and Mo-CBP3-PepIII Are Synthetic Antimicrobial Peptides Active against Human Pathogens by Stimulating ROS Generation and Increasing Plasma Membrane Permeability. *Biochimie* **2019**, *157*, 10−21.

(12) Souza, P. F. N.; Marques, L. S. M.; Oliveira, J. T. A.; Lima, P. G.; Dias, L. P.; Neto, N. A. S.; Lopes, F. E. S.; Sousa, J. S.; Silva, A. F. B.; Caneiro.; et al. Synthetic Antimicrobial Peptides: From Choice of the Best Sequences to Action Mechanisms. *Biochimie* **2020**, *175*, 132−145.

(13) Stockert, J. C.; Horobin, R. W.; Colombo, L. L.; Blázquez-Castro, A. Tetrazolium Salts and Formazan Products in Cell Biology: Viability Assessment, Fluorescence Imaging, and Labeling Perspectives. *Acta Histochem.* **2018**, *120*, 159−167.

(14) Abu-Raddad, L. J.; Chemaitelly, H.; Butt, A. A. Effectiveness of the BNT162b2 Covid-19 Vaccine against the B.1.1.7 and B.1.351 Variants. *N. Engl. J. Med.* **2021**, *385*, 187.

(15) Heath, P. T.; Galiza, E. P.; Baxter, D. N.; Boffito, M.; Browne, D.; Burns, F.; Chadwick, D. R.; Clark, R.; Cosgrove, C.; Galloway, J.; et al. Safety and Efficacy of NVX-CoV2373 Covid-19 Vaccine. *N. Engl. J. Med.* **2021**, *385*, 1172.

(16) Gupta, R. K. Will SARS-CoV-2 Variants of Concern Affect the Promise of Vaccines? *Nat. Rev. Immunol.* **2021**, *21*, 340−341.

(17) Coronavirus (COVID-19) Vaccinations - Statistics and Research - Our World in Data https://ourworldindata.org/covid-vaccinations (accessed Jul 15, 2021).

(18) Mathieu, E.; Ritchie, H.; Ortiz-Ospina, E.; Roser, M.; Hasell, J.; Appel, C.; Giattino, C.; Rodés-Guirao, L. A Global Database of COVID-19 Vaccinations. *Nat. Hum. Behav.* **2021**, *5*, 947−953, DOI: 10.1038/S41562-021-01122-8.

(19) COVID-19 Breakthrough Case Investigations and Reporting | CDC https://www.cdc.gov/vaccines/covid-19/health-departments/breakthrough-cases.html (accessed Jul 15, 2021).

(20) What You Should Know About the Possibility of COVID-19 Illness After Vaccination|CDC https://www.cdc.gov/coronavirus/2019-ncov/vaccines/effectiveness/why-measure-effectiveness/breakthrough-cases.html (accessed Jul 15, 2021).

(21) COVID-19 Vaccines Advice https://www.who.int/emergencies/diseases/novel-coronavirus-2019/covid-19-vaccines/advice (accessed Jul 15, 2021).

(22) Elfiky, A. A. Ribavirin, Remdesivir, Sofosbuvir, Galidesivir, and Tenofovir against SARS-CoV-2 RNA Dependent RNA Polymerase (RdRp): A Molecular Docking Study. *Life Sci* **2020**, *253*, 117592.

(23) Vankadari, N. Arbidol: A Potential Antiviral Drug for the Treatment of SARS-CoV-2 by Blocking Trimerization of the Spike Glycoprotein. *Int. J. Antimicrob. Agents* **2020**, *56*, 105998.

(24) Wang, X.; Cao, R.; Zhang, H.; Liu, J.; Xu, M.; Hu, H.; Li, Y.; Zhao, L.; Li, W.; Sun, X.; Yang, X.; et al. The Anti-Influenza Virus Drug, Arbidol Is an Efficient Inhibitor of SARS-CoV-2 in Vitro. *Cell Discov.* **2020**, *6*, 1−5.

(25) Yang, C.; Ke, C.; Yue, D.; Li, W.; Hu, Z.; Liu, W.; Hu, S.; Wang, S.; Liu, J. Effectiveness of Arbidol for COVID-19 Prevention in Health Professionals. *Front. Public Health* **2020**, *0*, 249.

(26) Sacramento, C. Q.; Fintelman-Rodrigues, N.; Temerozo, J. R.; et al. In Vitro Antiviral Activity of the Anti-HCV Drugs Daclatasvir and Sofosbuvir against SARS-CoV-2, the Aetiological Agent of COVID-19. *J. Antimicrob. Chemother.* **2021**, *76*, 1874−1885.

(27) Wang, M.; Cao, R.; Zhang, L.; Yang, X.; Liu, J.; Xu, M.; Shi, Z.; Hu, Z.; Zhong, W.; Xiao, G. Remdesivir and Chloroquine Effectively Inhibit the Recently Emerged Novel Coronavirus (2019-NCoV) in Vitro. *Cell Res.* **2020**, *30*, 269−271.

(28) Beigel, J. H.; Tomashek, K. M.; Dodd, L. E.; Mehta, A. K.; Zingman, B. S.; Kalil, A. C.; Hohmann, E.; Chu, H. Y.; Luetkemeyer, A.; Kline, S.; et al. Remdesivir for the Treatment of Covid-19 — Final Report. *N. Engl. J. Med.* **2020**, *383*, 1813−1826.

(29) Curreli, A. F.; Victor, S. M. B.; Ahmed, S.; Drelich, B.; Tong, X.; Chien-Te, K.; Tseng, C. D. H.; Debnatha, A. K. Stapled Peptides Based on Human Angiotensin-Converting. *mBio* **2020**, *11*, 1−13.

(30) Larue, R. C.; Xing, E.; Kenney, A. D.; Zhang, Y.; Tuazon, J. A.; Li, J.; Yount, J. S.; Li, P. K.; Sharma, A. Rationally Designed ACE2-Derived Peptides Inhibit SARS-CoV-2. *Bioconjugate Chem.* **2021**, *32*, 215−223.

(31) Han, S.; Zhao, G.; Wei, Z.; Chen, Y.; Zhao, J.; He, Y.; He, Y. J.; Gao, J.; Chen, S.; Du, C.; et al. An Angiotensin-Converting Enzyme-2-Derived Heptapeptide GK-7 for SARS-CoV-2 Spike Blockade. *Peptides* **2021**, *145*, 170638.

(32) FDA. *Fact Sheet For Healthcare Providers G Medical Vsms Ecg Patch*, 2020.

(33) Adamsick, M. L.; Gandhi, R. G.; Bidell, M. R.; Elshaboury, R. H.; Bhattacharyya, R. P.; Kim, A. Y.; Nigwekar, S.; Rhee, E. P.; Sise, M. E. Remdesivir in Patients with Acute or Chronic Kidney Disease and COVID-19. *J. Am. Soc. Nephrol.* **2020**, *31*, 1384−1386.

(34) Wang, M.; Shu, B.; Bai, W.-X.; Liu, J.; Yao, J. A 4-Week Oral Toxicity Study of an Antiviral Drug Combination Consisting of Arbidol and Acetaminophen in Rats. *Drug Chem. Toxicol.* **2010**, *33*, 244−253.

(35) Fan, Q.; Zhang, B.; Ma, J.; Zhang, S. Safety Profile of the Antiviral Drug Remdesivir: An Update. *Biomed. Pharmacother.* **2020**, *130*, 110532.

(36) MacRae, C. A.; Peterson, R. T. Zebrafish as Tools for Drug Discovery. *Nat. Rev. Drug Discovery* **2015**, *14*, 721−731.

(37) Zhang, T.; Chen, Z.; Tian, Y.; Han, B.; Zhang, N.; Song, W.; Liu, Z.; Zhao, J.; Liu, J. Kilogram-Scale Synthesis of Osteogenic Growth Peptide (10-14) Using a Fragment Coupling Approach. *Org. Process Res. Dev.* **2015**, *19*, 1257−1262.

(38) Pennington, M. W.; Zell, B.; Bai, C. J. Commercial Manufacturing of Current Good Manufacturing Practice Peptides Spanning the Gamut from Neoantigen to Commercial Large-Scale Products. *Med. Drug Discovery* **2021**, *9*, 100071.

(39) Buckley, S. T.; Bækdal, T. A.; Vegge, A.; Maarbjerg, S. J.; Pyke, C.; Ahnfelt-Rønne, J.; Madsen, K. G.; Schéele, S. G.; Alanentalo, T.; Kirk, R. K.; et al. Transcellular Stomach Absorption of a Derivatized Glucagon-like Peptide-1 Receptor Agonist. *Sci. Transl. Med.* **2018**, *10*, 7047.

(40) Holshue, M. L.; DeBolt, C.; Lindquist, S.; Lofy, K. H.; Wiesman, J.; Bruce, H.; Spitters, C.; Ericson, K.; Wilkerson, S.; Tural, A.; et al. First Case of 2019 Novel Coronavirus in the United States. *N. Engl. J. Med.* **2020**, *382*, 929−936.

(41) Harcourt, J.; Tamin, A.; Lu, X.; Kamili, S.; Sakthivel, S. K.; Murray, J.; Queen, K.; Tao, Y.; Paden, C. R.; Zhang, J.; Li, Y.; et al. Severe Acute Respiratory Syndrome Coronavirus 2 from Patient with Coronavirus Disease, United States - Volume 26, Number 6—June 2020 - Emerging Infectious Diseases Journal - CDC. *Emerg. Infect. Dis.* **2020**, *26*, 1266−1273.

(42) Mendoza, E. J.; Manguiat, K.; Wood, H. Two Detailed Plaque Assay Protocols for the Quantification of Infectious SARS-CoV-2. *Curr. Protoc. Microbiol.* **2020**, *57*, cpmc105.

(43) López-Martínez, R.; Ramírez-Salinas, G. L.; Correa-Basurto, J.; Barrón, B. L. Inhibition of Influenza A Virus Infection In Vitro by Peptides Designed In Silico. *PLoS One* **2013**, *8*, No. e76876.

(44) Muruato, A. E.; Fontes-Garfias, C. R.; Ren, P.; Garcia-Blanco, M. A.; Menachery, V. D.; Xie, X.; Shi, P.-Y. A High-Throughput Neutralizing Antibody Assay for COVID-19 Diagnosis and Vaccine Evaluation. *Nat. Commun.* **2020**, *11*, 1−6.

(45) Lamiable, A.; Thévenet, T.; Rey, R.; Vavrusa, M. PEP-FOLD3: Faster de Novo Structure Prediction for Linear Peptides in Solution and in Complex. *Nucleic Acids Res.* **2016**, *44*, W449−W454.

(46) Martínez-Rosell, G.; Giorgino, T.; De Fabritiis, G. PlayMolecule ProteinPrepare: A Web Application for Protein Preparation for Molecular Dynamics Simulations. *J. Chem. Inf. Model.* **2017**, *57*, 1511−1516.

(47) Kozakov, D.; Hall, D. R.; Xia, B.; Porter, K. A.; Padhorny, D.; Yueh, C.; Beglov, D.; Vajda, S. The ClusPro Web Server for Protein−Protein Docking. *Nat. Protoc.* **2017**, *12*, 255−278.

(48) Lensink, M. F.; Nadzirin, N.; Velankar, S.; Wodak, S. J. Modeling Protein-protein, Protein-peptide, and Protein-oligosaccharide Complexes: CAPRI 7th Edition. *Proteins: Struct., Funct., Bioinf.* **2020**, *88*, 916−938.

(49) Laskowski, R. A.; Swindells, M. B. LigPlot+: Multiple Ligand−Protein Interaction Diagrams for Drug Discovery. *J. Chem. Inf. Model.* **2011**, *51*, 2778−2786.

(50) T, M. Rapid Colorimetric Assay for Cellular Growth and Survival: Application to Proliferation and Cytotoxicity Assays. *J. Immunol. Methods* **1983**, *65*, 55−63.

(51) Collins, A. R. The Comet Assay for DNA Damage and Repair: Principles, Applications, and Limitations. *Mol. Biotechnol.* **2004**, *26*, 249−261.

(52) Burlinson, B.; Tice, R. R.; Speit, G.; Agurell, E.; Brendler-Schwaab, S. Y.; Collins, A. R.; Escobar, P.; Honma, M.; Kumaravel, T. S.; et al. Fourth International Workgroup on Genotoxicity Testing: Results of the in Vivo Comet Assay Workgroup. *Mutat. Res. Genet. Toxicol. Environ. Mutagen* **2007**, *627*, 31−35.

(53) McGahon, A. J.; Martin, S. J.; Bissonnette, R. P.; Mahboubi, A.; Shi, Y.; Mogil, R. J.; Nishioka, W. K.; Green, D. R. Chapter 9 The End of the (Cell) Line: Methods for the Study of Apoptosis in Vitro. *Methods Cell Biol.* **1995**, *46*, 153−185.

(54) Test No. 236: Fish Embryo Acute Toxicity (FET) Test | READ online https://read.oecd-ilibrary.org/environment/test-no-236-fish-embryo-acute-toxicity-fet-test_9789264203709-en#page1 (accessed Jul 12, 2021).

(55) Muniz, M. S.; Halbach, K.; Alves Araruna, I. C.; Martins, R. X.; Seiwert, B.; Lechtenfeld, O.; Reemtsma, T.; Farias, D. Moxidectin Toxicity to Zebrafish Embryos: Bioaccumulation and Biomarker Responses. *Environ. Pollut.* **2021**, *283*, 117096.